Dissipation around Rolling Boxes

Lin LU[1, 3], Xiaobo CHEN[2], Bin TENG[3], Ying GOU[3], Shengchao JIANG[3] and Xiaoling GUO[3]

[1]Center for Deepwater Engineering, Dalian University of Technology, Dalian 116024, China
LuLin@dlut.edu.cn
[2] Research Department, Bureau Veritas, Neuilly-Sur-Seine92570, France
[3] State Key Laboratory of Coastal and Offshore Engineering, Dalian University of Technology, Dalian 116024, China

Introduction

Potential flow theory is widely used in ocean hydrodynamics. With the great progress achieved so far, the weakness of the conventional potential flow model was also found for some special problems. One of the typical examples is the gap resonance, where the unexpected extremely large wave amplitude in the narrow gap, confined by the floating structures arranged side-by side, is predicted by the conventional potential flow model. The over-prediction of wave amplitude by the potential flow model near the resonant frequency is also observed for the liquid sloshing in a container. As far as ship motions in ocean wave are concerned, the rolling damping remains still great challenge for the potential flow theory. Empirical coefficients associated with the rolling damping are generally required in practical applications in order to make reasonable predictions of ship motions.

The gap resonance, sloshing and rolling problems mentioned above present a common characteristic, that is, the physical dissipation plays an important and critical role. However, *the conventional potential flow model is based on two basic assumptions of irrotational flow and inviscid fluid*, which means that the physical dissipation in the fluid flow has to be totally ignored. Therefore the conventional potential flow model becomes invalid for the cases with significant mechanical energy dissipation. In the context of viscous fluid flow with incompressibility, on the other hand, the mechanical energy dissipation can be described by the dissipation rate function from the energy equation,

$$\Psi = 2\mu s_{ij} s_{ij} \tag{1}$$

where μ stands for the fluid viscosity and s_{ij} = 0.5 ($\partial u_i/\partial x_j + \partial u_j/\partial x_i$) for the strain rate tensor with u_i the flow velocity component. Eq. (1) denotes the work rate dissipated in unit volume, having a dimension of [$JS^{-1}L^{-3}$]. The dissipation function can be re-formulated by subtracting the continuity equation $2(\partial u_i/\partial x_j)^2 = 0$, which leads to[1]

$$\Psi = \mu\omega^2 + 4\mu\left(\frac{\partial u}{\partial y}\frac{\partial v}{\partial x} - \frac{\partial u}{\partial x}\frac{\partial v}{\partial y}\right) \tag{2}$$

for the two-dimensional situation, where ω is the vortice and u, v the velocity components in the 2-D case.

As for the potential flow, the vortices are definitely zero. Furthermore, if the fluid is ideal, no dissipation is produced since the viscosity is zero. However, if we consider the special case of irrotational (potential) flows of viscous fluids, that is, *the viscous potential flow*, the dissipation function might be not zero since the second term in the right hand of Eq. (2) has to be retained. Note that the viscous fluid flow can be irrotational flow [2]. Considering the Helmholtz Theorem, that is,

$$\mathbf{u} = \nabla\Phi + \mathbf{v} \tag{3}$$

where $\mathbf{u}$ is the velocity vector, Φ the velocity potential, giving $\nabla\Phi$ the irrotational velocity and $\mathbf{v}$ the rotational part of the velocity, Joseph et al (2006)[3] presented the integral dissipation function in space

$$\begin{aligned}\Theta = \int_V 2\mu s_{ij} s_{ij} dV &= 2\mu\int_V \frac{\partial^2\Phi}{\partial x_i \partial x_j}\frac{\partial^2\Phi}{\partial x_i \partial x_j} dV \\ &+ \frac{\mu}{2}\int_V \left(\frac{\partial v_i}{\partial x_j} + \frac{\partial v_j}{\partial x_i}\right)\left(\frac{\partial v_i}{\partial x_j} + \frac{\partial v_j}{\partial x_i}\right) dV \\ &+ 2\mu\int_V \left(\frac{\partial v_i}{\partial x_j} + \frac{\partial v_j}{\partial x_i}\right)\frac{\partial^2\Phi}{\partial x_j \partial x_j} dV\end{aligned} \tag{4}$$

The above dissipation function with Helmholtz decomposition shows that the energy dissipation is composed of three parts. The first one purely results from the potential flow (irrotational velocity components) $\Theta_p = 2\mu \int_\Omega \Phi_{,ij}\, \Phi_{,ij}\, d\Omega$ and the second part comes from the rotational velocity components, $\Theta_v = 0.5\mu \int_\Omega (v_{i,j} + v_{j,i})^2\, d\Omega$ while the third part due to the coupling effect of potential flow and rotational flow gives rise to $\Theta_{p\sim v} = 2\mu \int_\Omega (v_{i,j} + v_{j,i})\, \Phi_{i,j}\, d\Omega$. Eq. (4) indicates clearly that the potential flow of viscous fluid is able to partially consider the mechanical energy dissipation although the potential dissipation might be limited for the real-life problems.By using the Gauss theorem and considering the boundary conditions of potential flow of viscous fluids, the potential dissipation Θ_p can be transformed to the boundary integral[4],

$$\Theta_p = 2\mu\int_{Sf} \frac{\partial^2\Phi}{\partial \mathbf{n}^2} u_n ds + 2\mu\int_{Sf} \frac{\partial u_n}{\partial \boldsymbol{\tau}} u_\tau ds \tag{5}$$

Where $u_n = \partial\Phi/\partial\mathbf{n}$, $u_\tau = \partial\Phi/\partial\boldsymbol{\tau}$ with $\mathbf{n}$ and $\boldsymbol{\tau}$ the unit vectors in normal and tangent directions, respectively, and *sf* stands for the free surface boundary. Eq. (5) indicates that the energy dissipation of viscous potential flow appears along the free surface, which can be regarded as the theoretical foundation for our previous method by introducing damping term on the free surface for the gap resonance problem [5, 6]. It should be pointed out that the governing equations of mass conservation and momentum conservation are the same for the potential flows of both ideal fluid and viscous fluid, i.e., the Laplace equation and Bernoulli equation. The details of the viscous potential flow theory can be found in Ref. [4].

The introduction of the concept of viscous potential flow provides us a feasible approach to consider the dissipation in the frame of potential flow theory. However, the energy dissipation in realistic flows may involve significant vortical (rotational) contributions, and the dissipation will not be restricted to the free surface. Therefore, it is necessary to know well *where dissipation mainly appears and how much dissipation is for a special problem*. This is the main issue of the present work by examining the rolling dissipation in fluid. In the following section, the dissipation of a rotationally oscillating square box in viscous fluid will be examined by the CFD simulations. We consider one submerged box first and one floating box with free-surface effect as another case.

Submerged box rolling in closed container

The governing equation is the two-dimensional Navier-Stokes equations for incompressible viscous fluid in the Arbitrary- Lagrangian-Eulerian frame,

$$\frac{\partial u_i}{\partial x_i} = 0 \tag{6}$$

$$\frac{\partial u_i}{\partial t} + \left(u_j - c_j\right)\frac{\partial u_i}{\partial x_j} = -\frac{1}{\rho}\frac{\partial p}{\partial x_i} + \frac{\mu}{\rho}\frac{\partial}{\partial x_j}\frac{\partial u_i}{\partial x_j} \tag{7}$$

where u_i and c_j are the fluid velocity and mesh velocity components corresponding to the i-th Cartesian coordinate x_i (i=1, 2 for the present 2-D problem), p the pressure, t the time and the liquid density ρ = 1000 kg/m^3 is used in this work. For the purpose to understand well the influence of fluid viscosity the heavy dynamic viscosity μ = 10.0 kg/m·s is adopted here. A rectangular box with square cross-section in *x-o-y* plan (with side length D =1.0 m) is placed in a closed square container fully filled with liquid. The rolling motion of the square cylinder is described by the forced rotational oscillation with respect to its centre, coinciding with the centre of the container.

$$\theta(t) = \theta_0 \sin\left(2\pi ft\right) \tag{8}$$

where θ is the time-dependent rotational angle in radian, θ_0 the amplitude and f the frequency in Hz. A sketch definition for the submerged square cylinder in a typical computational domain 40D×40D is shown in Fig. 1.

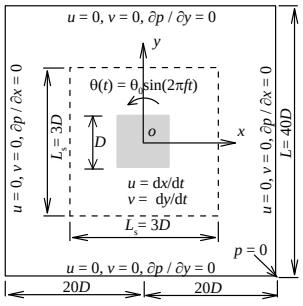

Fig. 1 Sketch definition of submerged rolling box

The no-slip boundary condition is applied on the solid wall, including the box surface and container boundary and a zero reference pressure is imposed at the down-right corner of the container.

The numerical model is firstly verified with different grid resolutions. It is confirmed that the computational meshes is fine enough, giving that the numerical results are free from the mesh density.That means the numerical dissipation is ignorable comparing with the physical dissipation. The influences of container size, fluid viscosity, rolling amplitude and frequency on the mean energy dissipation rate, denoted by Ξ, are concerned, which is evaluated as

$$\Xi = \frac{1}{T_2 - T_1}\int_{T_1}^{T_2} \Theta dt = \frac{1}{T_2 - T_1}\int_{T_1}^{T_2}\int_V 2\mu s_{ij} s_{ij} dV dt \tag{8}$$

where T_1 and T_2 is the integral time scale covering the stable state. Three different container sizes, measured by the container side length L = 20D, 40D and 60D, are examined with fixed rotation frequency f = 1.0 Hz and amplitude θ_0 = 0.1 rad. The numerical results show that the mean energy dissipation rates in the whole fluid domain confined by the different container sizes hold the same value of 6.255 J/s. This suggests that wall effects from the container on the dissipation can be neglected for the present numerical set-up, in other words, the dissipation rate induced by the container boundaries approaches to zero, giving the reasonable assumption with infinite computational domain. Therefore, the medium container size L = 40D×40D is adopted as the benchmark for the following computations.

As mentioned previously, one of the concerned issues for the dissipation is to get know where the dissipation takes place. We evaluated the mean dissipation rate in several square regions with respect to the rotation centre, i.e., L_s = 1.0D, 1.6D, 2.0D, 3.0D, 4.0D, 10.0D, 20.0D, 30.0D and 40.0D, referring to the definition in Fig. 1. The other computational parameters include μ = 10 kg/m·s, ρ = 1000 kg/m^3, θ_0 = 0.1 rad and $f\in$ [0.1, 1.0] with an increment of 0.1 Hz. As shown in Fig. 2, the increase in the area of the sub-domain does not increases the dissipation rate significantly. That means the mechanical energy dissipation mainly happens in the near region of the rolling box. Careful examinations indicate that the area of 3.0D×3.0D may account for more than 90% dissipation of the whole fluid domain for the present cases. Fig. 2 suggests also that the dissipation rate increases approximately in parabolic with the rolling frequency at constant rolling amplitude, which means the higher frequency gives the larger dissipation.

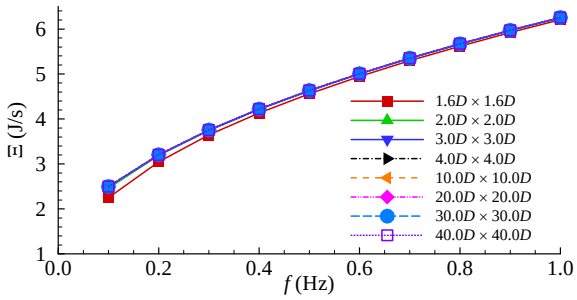

Fig. 2 Variation of mean dissipation rate with rolling frequency within different sub-domain size

Fig. 3 presents the comparisons of the dissipation rates under various rolling amplitudes. The mean dissipation rate is evaluated in the typical two sub-domains of 3.0D×3.0D and 20.0D×20.0D. It can be seen that the rolling amplitude has significant influence on the mean dissipation rate. For a particular frequency, the larger rolling amplitude gives rise to the higher dissipation at a rate larger than linear increase.

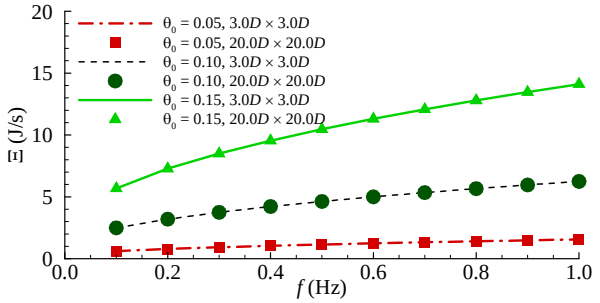

Fig. 3 Comparison of mean dissipation rate under different rotation amplitude

Fluid viscosity is expected to play important role in the mechanical energy dissipation, which is examined in Fig. 4 by considering the various viscosities at constant rolling amplitude θ_0 = 0.1 rad and frequency f = 0.4 Hz. This figure shows that the total dissipation in the fluid domain does not behave a linear increase with the fluid viscosity although the viscosity in Eq. (1) presents in linearity. Fig. 4 implies the importance of velocity gradient (mainly accounted by the vortices).

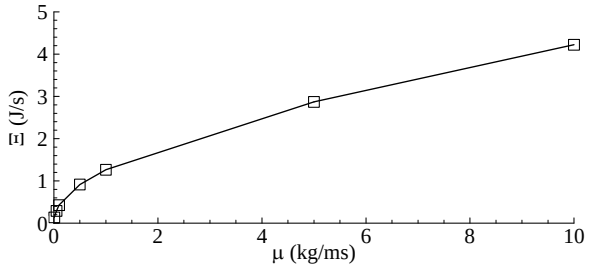

Fig. 4 Influence of fluid viscosity on dissipation

Based on the CFD numerical results the correlation between the dissipation and vortices are examined in Fig. 5 for typical θ_0 = 0.15 rad and f = 0.1 Hz. It can be observed that the total dissipation shown in Fig. 5 (left), by using Eq. (1), mainly appears in the near region of the rolling box and the most significant energy dissipations appear around the sharp corners. The dissipation resulted from the vortex motion in Fig. 5 (middle), evaluated by the first term of the right hand of Eq. (2), presents the similar scenery to that of Fig. 5 (left). The further examination in quantity indicates that the vortices dissipation accounts for most of the total dissipation. From Fig. 5 (right), it is confirmed that the vortices mainly develop from the solid wall and the sharp corners. The numerical results shown in Fig. 5 suggest that the dissipation induced by the vortical flow has to be modeled in order to use the viscous potential flow theory to successfully describe the rolling damping. Two points should be addressed, 1) the physical dissipation should be introduced near to the rolling structure and 2) the appropriate dissipation amount should be used. One feasible method for the former topic might be the dissipative surface idea proposed by Chen et al (2011)[7] while the latter one can be estimated by using the CFD simulations as described in this work.

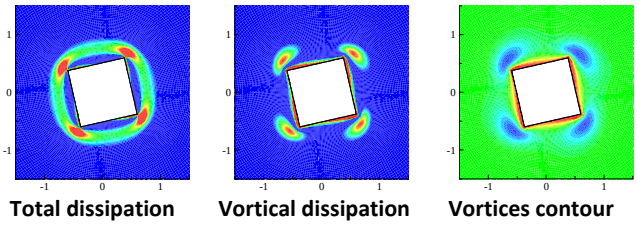

Fig. 5 Contours of dissipation rates and vortices

Floating box on free surface

By using the Navier-Stokes solver involving two-phase fluids, the rolling dissipation with free surface was simulated, where the liquid-gas interface is capture by the Volume of Fluid method. For the purpose of comparison, the computational domain, box size, rotationally oscillating amplitudes and frequencies are set to be as close as those in the previous section. The container is partially filled with liquid in a depth of 20D, i.e., half of the vertical dimension. The viscosities and densities used in the computations for the liquid and gas phases are μ_L= 10.0 kg/m·s, ρ_L = 1000 kg/m^3 and μ_A= 10^{-5} kg/m·s, ρ_A = 1.0 kg/m^3, respectively.

The time-series of wave elevations recorded at x = 1.0m, 5.0m, 10.0m and 20.0m, respectively, are shown in Fig. 6 for the case with f = 0.5 Hz and θ_0 = 0.1 rad. It shows that the wave amplitude decreases with the increase in the distance. At x = 10 m, the wave amplitude approaches to 1/6 of that at x =1.0 m and the wave energy is totally damped out at x = 20.0 m. The further examinations show that the higher oscillating frequency leads to the faster decrease in the wave height with the distance.

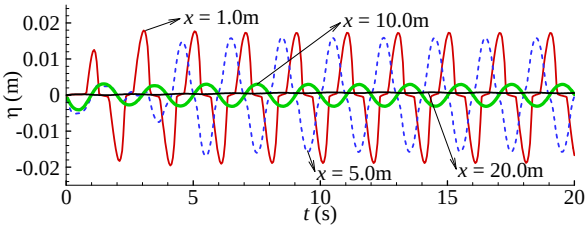

Fig. 6 Time series of wave elevation at different position

Eq. (2) suggests that the total dissipation rate consists of two parts, i.e., the first term and the second term on the right hand, which are denoted by the vortical dissipation rate and the other dissipation rate, respectively. The time evolutions of dissipation rates in the whole domain are examined in Fig. 7, for the case of f = 1.0 Hz and θ_0 = 0.1 rad, where the space integral over both the liquid and gas phases are involved. Since the gas viscosity is much smaller than the liquid, it is confirmed to have rather limited contribution to the total dissipation. It can be seen that the total dissipation rate ($\int_\Omega \Psi d\Omega$) is

mainly resulted from the vortical flow ($\int_\Omega \mu\omega^2 d\Omega$). For the present case the dissipation rate induced by the second term of Eq. (2), i.e., $\int_\Omega 4\mu\,(u_y v_x - u_x v_y)\,d\Omega$, accounts for 10% of the total dissipation rate, in which both potential and vortical dissipations and their coupling effects are all involved according to the previous mentioned Helmholtz decomposition in Eq. (4).

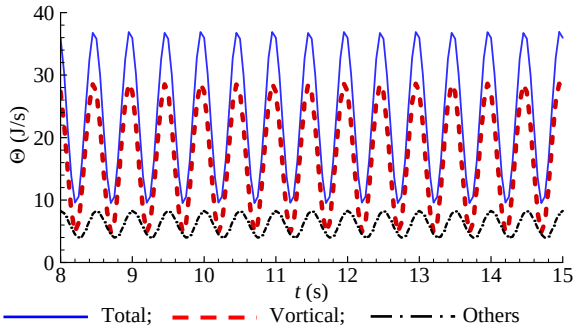

Fig. 7 Time series of dissipation rates in the whole domain

Following the previous examinations, the mean dissipation rates in various sub-domains with different square size are compared in Fig. 8, which is helpful to determine the most significantly dissipative region. The rotational amplitude and frequency considered here are 1.0 Hz and 0.1 rad, respectively. Note that the square sub-domains with side length L_s cover both of the liquid and gas regions and the three types of mean dissipation rate are considered. The numerical results show that the mean total dissipation, evaluated directly from Eq. (8), increases with the sub-domain size. However, as $L_s > 15$ m, that is, 15D in this work, the total mean dissipation rate approaches constant. That means the physical dissipation is mainly restricted in the scope of 15D×15D, which is much larger than the previous examined cases of submerged rolling box due to the presence of free surface. Again, the dissipation is observed to be mainly induced by the vortical flow. However, the mean vortical dissipation rate shows little dependence on the sub-domain size. As the sub-domain is large enough, the other dissipations account for nearly 25% of the total dissipation.

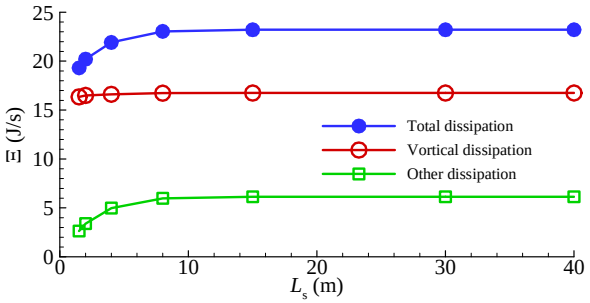

Fig. 8Mean dissipation rate in different sub-domain

The influence of rotational frequency on the mean dissipation rates in the whole domain are examined in Fig. 9 by considering the typical example with $\theta_0 = 0.1$ rad. It was found that at the lower frequencies the mean dissipation rate associated with the second term in Eq. (2) is very small while the total mean dissipation rate is almost the same as that from the vortical flow. With the increase in the frequency, the three dissipation rates increase gradually, and the difference between the total dissipation and the vortical dissipation becomes evident, which means the dissipation induced by the third term of Eq. (2) plays more and more important role at the higher oscillating frequencies.

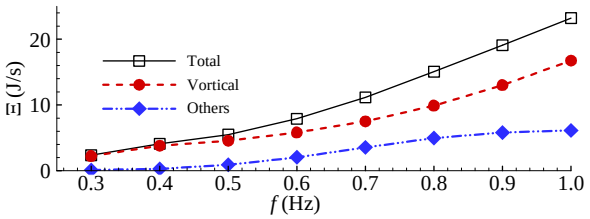

Fig. 9 Dependence of dissipation rate on rolling frequency

Conclusion

For the purpose to introduce dissipation in potential flows to deal with the near resonant problems in ocean engineering, we have performed analyses on the dissipation in viscous fluid and investigated quantitatively different components in the case of rolling boxes by using the CFD method. Two cases relative to one submerged box and one floating box at the free surface have been considered. The numerical results of dissipation rates associated with different components by varying rolling frequency and amplitude highlight that the major dissipation is contributed by fluid vortices in the region close to boxes. Further studies are needed to quantify the linear and quadratic coefficients of dissipation associated with rolling speed.

Acknowledgement

The finical supports from NSFC of China with granted Nos. 51279029and 51221961are acknowledged.

Reference

[1] Lamb H. 1945. *Hydrodynamics* (6th edition). Dover publication, New York, USA.

[2] Sirakov B T, Greitzer E M, Tan C S. 2005. A note on irrotational viscous flow.*Physics of Fluids*, 17, 108102.

[3] Joseph D. 2006. Helmholtz decomposition coupling rotational to irrotational flow of a viscous fluid.*PNAS*, 103 (39):14272-14277.

[4] Joseph D, Funada T, Wang J. 2008. *Potential Flows of Viscous and Viscoelastic Fluids*.Cambridge University Press.Cambridge, UK.

[5] Lu L, Teng B, Cheng L, Sun L, Chen XB. 2011a. Modelling of multi-bodies in close proximity under water waves — Fluid resonance in narrow gaps. *SCIENCE CHINA Physics, Mechanics & Astronomy*, 54 (1): 16-25.

[6]Lu L, Chen X B, TengB. 2012. Viscous dissipation and artificial damping for gap resonance problem.*Proceedings the 10th International Conference on Hydrodynamics (ICHD)*, Vol1, 257-262, October 1-4, St. Petersburg,

[7] Chen X B, Duan W Y, Liu H X. 2011. Dissipation effect in potential flows of fairly perfect fluid. *Proceedings of the 26th International Workshop on Water Waves and Floating Bodies (IWWWFB)*, 17-20 April, Athens, Greece.